CEAS Aeronautical Journal
https://doi.org/10.1007/s13272-022-00611-4

ORIGINAL PAPER

Inverter prototype development for HLFC compressor applications

Alexander Heinz Bismark[1] · **Patrick Juchmann**[1] · **Oliver Bertram**[1]

Received: 3 February 2022 / Revised: 18 July 2022 / Accepted: 17 August 2022

Abstract
A key component in Hybrid Laminar Flow Control (HLFC) is a turbo-compressor, which requires an inverter. However, a harsh environment in combination with restrictive boundary conditions make the inverter design very challenging. Moreover, aviation certification standards have to be considered. By reason of its growing significance, a Model-Based Systems Engineering (MBSE) approach is described to break the HLFC system requirements down to the lower level of the inverter. Using the acquired set of requirements, the design of an inverter prototype was initiated. For this, the compressor motor, a Permanent Magnet Synchronous Motor (PMSM) running up to 150,000 min^{-1} at a power of more than 5 kW, was characterized by measurements. Thereafter, a control concept was elaborated and implemented on a preliminary electronics. In the end, feasibility tests were conducted on a testbed, whose results match well with the theory.

Keywords Hybrid Laminar Flow Control · Model-Based Systems Engineering · Turbo-compressor · Inverter

1 Introduction

The European Green Deal sets high demands on the aviation industry by achieving climate neutrality until 2050 and targeting an emission reduction of more than 50 % in 2030, compared to 1990. Therefore, several airlines already committed to binding climate goals, for example by a fleet renewal and the use of new technologies. Those circumstances lead the Advisory Council for Aviation Research and Innovation in Europe (ACARE) to nudge an adaption of the FlightPath 2050 [1] while emphasizing the need to accelerate the technological progress towards decarbonisation.

Hybrid Laminar Flow Control (HLFC) is a promising technology to support this development. The approach is to suck air through a micro-perforated skin from the leading edge of an airfoil, so that the thickness of the boundary layer is reduced and curvature is changed. This stabilizes the laminar boundary layer and delays the laminar-turbulent transition. Hence, laminar flow length is increased leading to a decrease in drag, fuel consumption and emissions. This is not only beneficial from an environmental perspective, but also for economical reasons when considering the utilization of more expensive climate-neutral fuels such as bio-fuels or hydrogen in future.

HLFC has already been advanced in several projects, for example by wind-tunnel tests [2], flight tests [3, 4] or general design considerations [5–9]. Within the EU-funded Clean Sky 2 program, research is done for enabling HLFC on the Horizontal Tailplane (HTP) [10] and the wing [11] of an aircraft similar to the Airbus A330. In both projects, a compressor and its corresponding inverter are key elements to suck the air and thereby ensure the overall feasibility. This paper will focus on the inverter. However, past projects aimed to demonstrate the functionality of HLFC, but not to develop an economic overall solution. The suction system was always heavy and complex. Thus, there is no suitable state-of-the-art technology, which can be further developed. In addition, there is no equipment used in current serial aircraft production, which can be re-used for HLFC application.

Patrick Juchmann and Oliver Bertram authors contributed equally to this work.

✉ Alexander Heinz Bismark
Alexander.Bismark@dlr.de

Patrick Juchmann
Patrick.Juchmann@dlr.de

Oliver Bertram
Oliver.Bertram@dlr.de

[1] German Aerospace Center (DLR), Institute of Flight Systems, Lilienthalplatz 7, Braunschweig 38108, Lower Saxony, Germany

Published online: 17 September 2022

Inverters used for commercial application [12, 13], which are not certified for the use in aviation, are significantly larger than admitted for the system design. Additionally, liquid cooling is used, which is not practical for the integration in HLFC, for example due to tough space constraints. Therefore, a new inverter has to be designed to realize an economic HLFC solution, which shall be demonstrated on a representative compressor on the ground as an initial step. The challenges lie within the proper control of the compressor motor, a permanent magnet synchronous motor running up to 150,000 min^{-1}, as well as the high power (> 5 kW) that needs to be delivered by the inverter on a small allowable space allocation (max. 100 × 100 × 250 mm), which is challenging regarding a sufficient cooling of the inverter components.

Owing to the operation in an aviation environment, the applicable standards and procedures (e.g. ARP4754A, DO-160G) have to be met. Multi-functional components, which are integrated into HLFC as well, hold the potential to save weight and will, therefore, be more widely used in future aircraft. Though, system complexity is increased compared to a distributed architecture, where one component is assigned to a single function. This reveals limit of the classical approach [14] because functions are combined on one processing unit and can influence each other. Hence, Model-Based Systems Engineering (MBSE) gains importance to handle the complexity. According to this trend, a systematic method shall be applied to the inverter development utilizing MBSE. It provides a straightforward approach to integrate requirements from different domains and sources into one model. Due to the numerous standards and project boundary conditions to be considered in the design, MBSE aids to track all requirements, identify their sources and assure the appropriate implementation. Furthermore, features such as automatic verification or the implementation of simulations and assessments allow to centralize information in a multidisciplinary environment. Thereby, communication between different disciplines is eased as well. Though the application of MBSE to design a system is still a large research area and several aviation-related issues need to be tackled. This paper aims to describe a possible way of implementation. Figure 1 shows the inverter design approach, which is derived from the ARP4754A [15] and also in line with existing system design work [16–18].

In accordance with the process in Fig. 1, general requirements on the system level for the HLFC solution are described in Sect. 2.1 first. Based on that, Sect. 2.2 focuses on the elaboration of system functions and a generic architecture. Thereafter, the process of conducting the relevant safety assessments and the derivation of the corresponding requirements is explained (Sect. 2.3). In the end, the requirements and their sources are reviewed in Sect. 2.4 and the defined physical solution architecture is shown in

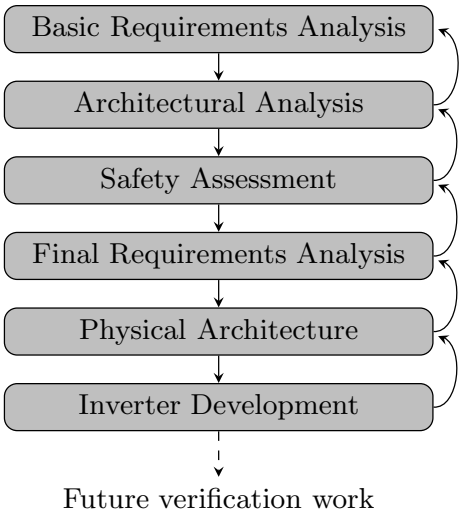

Fig. 1 Inverter design approach

Sect. 2.5. Generally, the goal was to break the requirements from system level down to lower levels to capture the applicable requirements for the inverter. This was necessary as low-level requirements were unknown in the beginning. The process was implemented in an MBSE model.

Based on the developed set of requirements, the inverter development is described in Sect. 3 for a given commercially available compressor. Due to the lack of data being crucial for the control of the compressor, the motor was at first characterized by measurements. Thereafter, a suitable control concept could be chosen and realized on an experimental testbed for initial testing. Future work will comprise the miniaturization of the current electronics and the implementation of all required functionalities.

2 Requirements breakdown process

Prior to the initiation of the component development, a systematic analysis process is introduced in order to capture all relevant requirements as well as developing a solution architecture. In general, all steps were realized in a model at Cameo Systems Modeler. However, the paper focuses on the process itself rather than showing the implementation in the model.

2.1 Stakeholder needs and overall requirements

The first step of development according to systems engineering methodology [19] is the identification of stakeholders and applicable standards for gathering relevant requirements. HLFC is allocated to the system level. Therefore, general requirements are inherited from aircraft level. The framework for this is given by the certification specifications

CS-25 [20], mainly in Subpart F (Equipment). Moreover, section AMC 25.1309 lists the applicable documents [15, 21–23] that should be considered to comply with the regulations. Consequently, requirements for the HLFC equipment were established in accordance with the corresponding categories defined in the DO-160G [22]. The elaboration of safety requirements and further related documents will be described in Sect. 2.3. It has to be noted that the DO-254 [24] is not explicitly listed in AMC 25.1309, but will nevertheless be mentioned later on.

Due to the work in a funded research project, the classical stakeholder relationship does not apply here. Instead, project guidelines and system requirements were defined within the consortium aiming to cover the needs of aviation industry participants, which would represent the key stakeholders. The most relevant requirements are listed in the following:

- The HLFC system shall be operable in cruise at a range between 33,000 ft and 41,000 ft,
- A mass flow of 600 g/s per wing shall be generated and 320 g/s per HTP side (preliminary aerodynamic calculations),
- Fuel savings generated by HLFC shall not be considered in the fuel planning,
- The Master Minimum Equipment List (MMEL) shall not be more restrictive than the comparative aircraft,
- Automatic and invisible system operation to the crew during flight shall be ensured unless there is a critical failure condition,
- In accordance with the More Electric Aircraft approach, voltages of 270 VDC and 28 VDC shall be used.

Based on these boundary conditions, an assessment for an optimized distribution of compressors was conducted as described in Ref. [10] containing a preliminary estimation for the HTP, too. However, due to a lower available space in the wing's leading edge as well as a spatial conflict with other systems (e.g. high-lift and ice protection system), the realization of HLFC is more challenging on the wing. As there shall be only one equipment version for the whole aircraft, the requirements for the compressor and inverter are, therefore, prescribed by the conditions on the wing.

The suction area extends outwards from the pylon in a spanwise direction on a length of 20 m and is divided into four segments of equal length (5 m). The spanwise distribution of compressors based on a preliminary system architecture assessment and the calculated mass flow values are shown in Fig. 2. Moreover, the HLFC system design based on the so-called ALTTA concept [2] is outlined in Fig. 3. An alternative approach is described in Ref. [25]. Main components for the chosen solution are the outer micro-perforated titanium skin, which is connected to the inner structure (carbon-fiber reinforced plastic) by spacers, as well as a

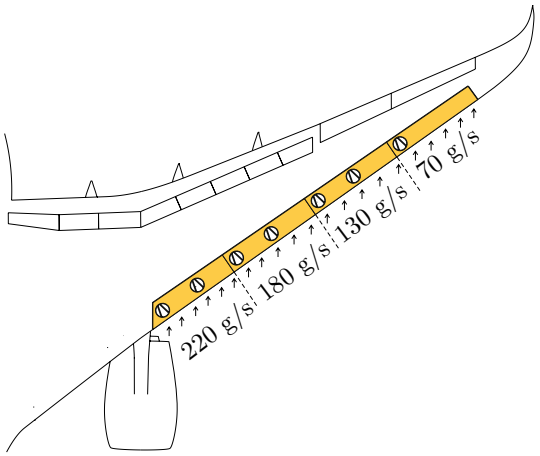

Fig. 2 Preliminary compressor and mass flow distribution

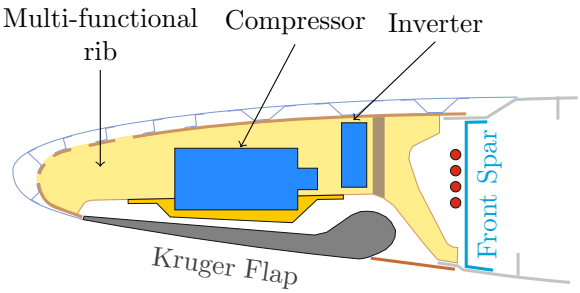

Fig. 3 Installation of HLFC System, Image courtesy: M. Kleineberg

sealed multi-functional rib. It is used as a structural rib and also comprises the suction system components (compressor, inverter and sensors). The preliminary design considers the sensors to be installed inside the compressor and inverter to reduce wiring effort and system complexity. However, the detailed compressor design will be investigated in a separate study.

Generally, a pressure drop is generated by the micro-perforated titanium skin. Thereafter, the air is transported through the chambers between the skin and structure to the multi-functional rib and reaches the compressor inlet by throttle holes in the structure. Moreover, the inverter is installed in the compressor inlet airflow to enhance air-cooling capabilities.

Apparently, the allowable space allocation for the suction system components strongly depends on the one provided by the multi-functional rib. Consequently, a maximum size for the inverter, which is discussed in this paper, of 100 × 100 × 250 mm was determined for the most constraining installation location. This refers to the most outboard segment as the leading edge narrows in spanwise direction. Nevertheless, to ensure the use of one equipment version only, it needs to be capable to drive a compressor on the maximum

required mass flow, which is the one for the most inboard segment (110 g/s per compressor, see Fig. 2). Hence, the maximum space is given by the outboard segment, whereas the required power is determined by the inboard segment. It has to be noted that the requirements on the wing also allow an installation on the HTP.

All requirements were incorporated into a model in the Cameo Systems Modeler, so that traceability can be assured and automatic verification is enabled later on. Additionally, appropriate subsystem and component requirements were derived from the ones previously given at the system level.

2.2 Functional decomposition and logical architecture

The definition of system functions is crucial for the development process. Firstly, it aids to ensure that the system performs all intended functions required by the stakeholders. Furthermore, it allows to elaborate a solution architecture by allocating logical components to the functions. In this way, a generic baseline is generated without specifying a designated solution. Based on that, different variants and their physical components can be developed and evaluated, as described in Ref. [19] and utilized [16–18]. The main function considered on the system level for this case is 'Provide HLFC'. Corresponding subsystem functions are shown on the left hand side in Fig. 4.

Following the process, logical components are allocated to the defined functions on the right hand side. In the Cameo Systems Modeler, this assignment is achieved by drawing the relations in a Block Definition Diagram (BDD). Thereafter, the logical architecture can be attributed to a solution architecture, which is shown in Fig. 5 for the elements being related to the inverter as this is the component considered in this paper.

Monitoring and air ingestion capabilities are assigned to the suction system consisting of the compressor, inverter and the required sensors. Monitoring in this case refers to the

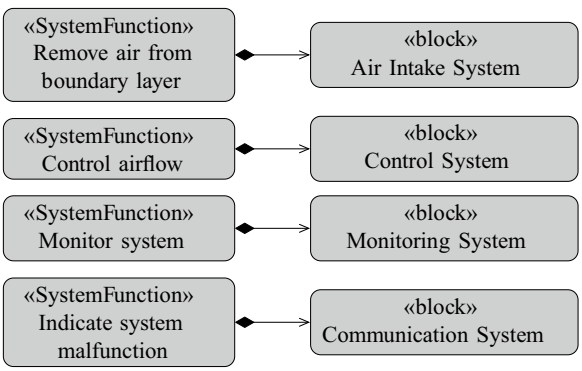

Fig. 4 Functional breakdown and logical architecture

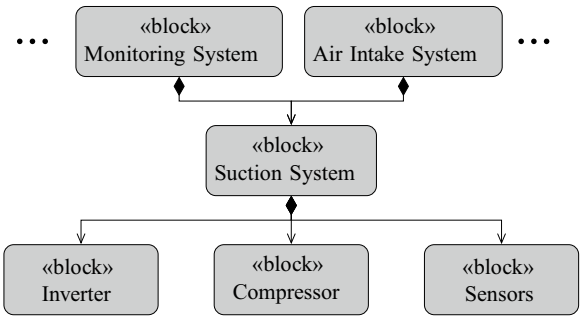

Fig. 5 Allocation of logical architecture to solution architecture for inverter-related elements

measurement of the air pressure, which is the input parameter for the control of the compressor speed, as well as parameters required to detect critical conditions (e.g. compressor overheat or rupture). Besides, it was defined that the control of the whole HLFC system will be realized by a central control computer located in the fuselage (not shown in Fig. 5).

The current project design introduces several compressors distributed along the span. To meet the total mass flow requirements as stated in the project guidelines, a mass flow of 110 g/s per compressor was derived from the system design, whereas each one is driven by its own inverter nearby. Moreover, communication between components of HLFC and other aircraft systems is handled by an Avionics Full DupleX Switched Ethernet (AFDX) bus. Hence, the inverter shall act as a decentralized electronics sending out sensor data on the bus to the control computer and receiving commands (e.g. compressor speed, start/stop) from it. Nevertheless, the inverter of course has to fulfill its purpose to drive the compressor. Those factors resulting from the solution architecture expand the set of requirements and are traced to its source in a Derive Requirement Matrix in Cameo. Further definitions of the physical architecture are made after additional constraints are set by the safety assessment. The following, descriptions will focus on the inverter and its intended functions.

2.3 Safety assessment

Conducting a safety assessment is usually not part of the systems engineering process, but crucial for the design of aviation equipment in accordance with the regulations. The ARP4754A defines the sequence of assessments to be carried out. In addition, the ARP4761 gives the guideline on how to conduct the assessments. Considering the preliminary design phase, the Functional Hazard Analysis (FHA), Preliminary System Safety Analysis (PSSA) and Common Cause Analysis (CCA) (see Ref. [15]) have to be taken into account.

To apply the FHA, functions defined in the functional breakdown are assessed for their criticality in case of a loss (total or partial) or incorrect working, where each failure condition can be detected or undetected. Furthermore, it has to be distinguished between a symmetric and asymmetric failure condition. Relating to the HLFC system, this indicates whether the failure occurs only on one wing (asymmetric) or on both sides (symmetric). However, the classification of safety effects does not differ in this case as an asymmetric failure would not lead to a significant degradation of flight safety compared to the symmetric case. A failure of HLFC basically increases the drag. Nevertheless, the asymmetric drag increase is small compared to the overall wing drag. Thus, this will result in a slight yaw moment only not being critical regarding flight safety.

By defining functions at different levels, the systems engineering process and the ARP4754A interlock well at this point. The failure conditions are classified according to their severity and the Functional Development Assurance Level (FDAL) is in turn assigned depending on the severity, architecture and in certain circumstances the probability of external events. Moreover, the FDAL dictates the guidelines to be followed during the design. The most decisive failure conditions for the suction system-related functions are shown in Table 1.

Due to the project directive that the fuel savings achieved by HLFC shall not be taken into account for the fuel planning, a loss or malfunction of the air ingestion capability has no safety effect. However, the monitoring could possibly cause a catastrophic effect on an initial estimation, so that the FDAL A applies. Owing to ARP4754A, all critical failures need to be evaluated in a PSSA. This is accomplished by conducting a Fault Tree Analysis (FTA). It has to be elaborated, which conditions might cause the top event. The case 'Incorrect function of monitoring' is depicted in Fig. 6 for demonstration purposes.

Having a look at the fault tree clarifies that single failure sources for the shown components are not permissible, which is required as well in the paragraph CS 25.1309. If for example there is only a simplex processing unit on the inverter producing an incorrect output, the whole monitoring function is corrupted. Hence, a second unit always needs to be implemented. Using this, a fail-safe behavior is achieved, which is reasonable as the loss of HLFC

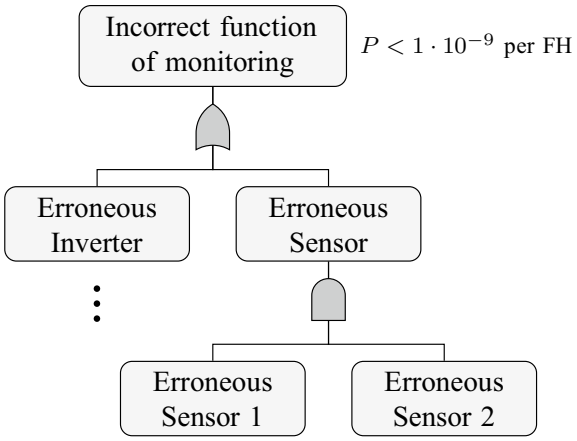

Fig. 6 Simplified FTA for 'Incorrect function of monitoring'

capabilities is not regarded critical. Hence, two sensors will be taken into account in the preliminary design. Using three sensors to achieve a fail-operational behavior will be assessed in future.

The 'Loss of monitoring' is not hazardous itself. It just has to be assured that the compressor can be properly deactivated in case the monitoring system experiences a partial or total loss. Applying the proposed architecture, this aspect is likewise covered.

Obviously, the FTA serves the design process in two ways. Firstly, it partly defines the physical architecture by revealing necessary safety measures such as redundancy. Secondly, an allowable failure rate can be assigned to each component to meet the required probability of failure. In case reliability data is already available, the system reliability can also be estimated on a preliminary basis. In this project, data from Ref. [26] and aviation manufacturers have been used to confirm that the design will probably meet the required reliability. However, the depicted process emphasizes the iterative character of system design and safety assessment, where findings from the analyses will be ascribed to the elaboration of solution candidates.

In the end, a CCA has to be conducted to eliminate failures resulting from the same source. The ARP4754A provides separate analysis methods for failure modes attributed to the same installation area, common external effects (e.g. lightning strike, foreign object damage) and the assurance

Table 1 FHA for critical suction system functions

Failure	Effect	Severity	Probability
Incorrect function of monitoring (undetected)	Operation out of limits, possible rupture or fire	Catastrophic	$< 1 \cdot 10^{-9}$per FH
Loss of monitoring (undetected)	Operation out of limits, possible rup- ture or fire	Catastrophic	$< 1 \cdot 10^{-9}$per FH

that failure events in the fault tree are independent from each other. Referring to the inverter, it was defined that wires of redundant sensors shall not be located within the same harness and end up in different connectors. Generally, sensor cables and power lines shall be separated at all time. To decouple the failure events of the fault tree, it is necessary to utilize dissimilar hardware and software on the inverter. Moreover, redundant sensors will be used to determine the monitoring data.

Up to now, the crucial safety assessments are not implemented yet in the Cameo Systems Modeler. For this reason, a plugin for the FHA was internally developed. System functions defined in the model are classified by the designer's expertise with regard to their criticality and manually assigned with the corresponding prescribed probability for their occurrence in case of a failure condition. Besides, sources for justifying the classification and diagrams for the verification can be linked to each hazard. In this way, an FHA table as required by the standards can be created.

For conducting the CCA, the Cameo Safety and Reliability Analyzer plugin was modified to suit the demands. The FTA should be part of the plugin in future, but for this work an external tool had to be used. In the Cameo model, a Requirement Diagram listing all derived safety requirements was created, where each requirement is traced to the element of the corresponding safety analysis.

Nevertheless, the classical procedures reach their limits on multi-functional and more complex avionics [14]. In order to tackle this issue, research is being made towards the Systems-Theoretic Process Analysis (STPA) as an alternative hazard analysis (e.g. [27, 28]). Moreover, the Object Management Group® released a beta version of the forthcoming Risk Analysis and Assessment Modeling Language (RAAML) [29] for promoting safety analyses, such as the STPA or FTA, in object-orientated languages. This would allow a more holistic approach for the design as all information can be captured and traced to each other in a single MBSE model.

2.4 Final requirements analysis

To start the elaboration of a suitable physical architecture, the set of requirements introduced in the course of the process should be reviewed in their entirety. In the previous section, the criticality was classified by the FHA, which also prescribes the efforts for the component development and certification process. Specific guidelines for this are given in the DO-254 [24] for hardware and DO-178C [23] for software. These have to be considered for the inverter development as well and extend the applicable requirements.

Requirements resulting from the DO-160G [22] were already implemented. The standard includes several environmental conditions (e.g. vibration, waterproofness), defines different categories and specifies corresponding tests depending on the operational conditions of the equipment. A categorization has been made for the compressor and inverter in the beginning.

Generally, a separate Requirement Diagram was created in the Cameo model for each level of detail down to the level of the inverter. Every requirement was linked to its source (e.g. DO-160G, project consortium) or the element from which it was derived (e.g. hazard element, superior requirement). Thereby, it can be checked that requirements are properly broken down to the relevant components and traceability is ensured.

Apart from the HLFC system, other technologies, e.g. an innovative anti-icing system or high-lift devices, are developed within the project. The multidisciplinary environment in turn strongly influences the boundary conditions. An increasingly detailed design or changes based on new findings within the project result in frequent adaptions of the suction system requirements. Utilizing MBSE, affected components can easily be identified as traceability is implemented in the Cameo model. Hence, it significantly eases the iterative process towards the design of the inverter suiting the combination of all systems. An overview of major sources taken into account for the final requirement analysis is shown in Fig. 7.

2.5 Physical architecture

The proposed analysis process ends in the definition of a physical inverter architecture, which sets the framework for the component design. As mentioned earlier, following the Integrated Modular Avionics (IMA) concept, the calculation of the desired compressor speed is realized by a centralized computer unit, whereas the inverter takes over the compressor control as well as the forwarding of sensor data being crucial for the monitoring of the suction system. In this way, it acts as a completely independent system with its own safety functions. Therefore, actions by the crew are not

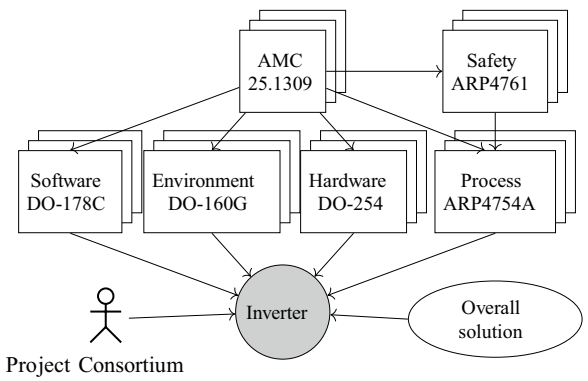

Fig. 7 Overview of requirement sources for the inverter

required during normal operation, as it is the case for example on the Full Authority Digital Engine Control (FADEC). The physical architecture based on the analysis is shown in Fig. 8 in the form of an BDD.

3 Component development

Having defined the solution architecture and requirements, the actual component design is initiated. In this case, a characterization of the compressor motor is crucial as adequate data was not available. Therefore, the type of electric motor was identified and a suitable control concept was chosen. To realize the control, certain motor parameters, such as phase inductivity, phase resistance or speed constant, need to be known. This was achieved by measuring the phase current and voltage during operation as well as tests in a static motor state using a LCR-meter. Moreover, the phase current, phase voltage and the voltage induced in the stator need to be continuously measured during operation to properly control the motor with the chosen concept.

Based on the findings, preliminary electronics were developed and verified on a testbed. The design aims to demonstrate the feasibility of driving the compressor first due to the challenging constraints. Afterwards, the inverter will be miniaturized to the allowable space allocation and required features such as the AFDX or dissimilar hardware will be implemented. However, this paper focuses on the target to realize a feasible control concept.

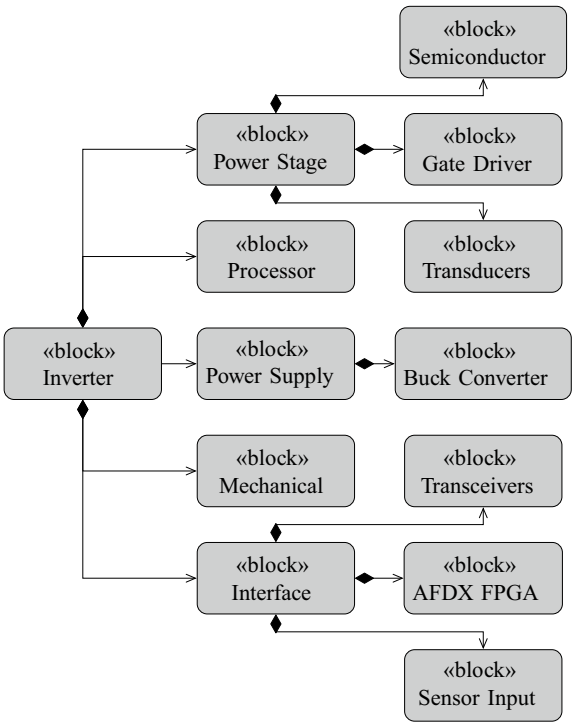

Fig. 8 Defined physical architecture for the inverter

3.1 Motor characterization

The chosen compressor is a commercially available lightweight radial turbo-compressor being used for ground tests of the HLFC system. However, as relevant parameters were not given in the data sheet, the motor characteristics of the compressor assembly had to be determined. This was done by an inline phase current and voltage measurement utilizing a high-frequency oscilloscope and corresponding measurement circuitry. Measurements were conducted with the inverter supplied by the compressor manufacturer at varying operating points including startup and shutdown. Furthermore, static measurements had been carried out to determine phase inductance and resistance values using an LCR-meter and a constant current source.

Figure 9 shows the base wave at a stationary point of operation at 25,000 min^{-1} for one phase. The base wave has a frequency of 416.6 Hz, which corresponds to the mechanical speed of the compressor, indicating a one-pole pair configuration. The voltage waveform showing a rather trapezoidal shape with a 60° pattern, which may result from sector changes within the voltage vector modulation.

Moreover, the speed constant can be approximated from the stationary base wave using the peak-to-peak phase voltage at the known mechanical speed. Since the star point of the motor was not accessible, the measured values presented in Table 2 are phase-to-phase values. The shown

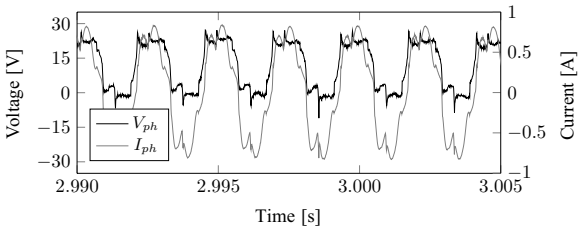

Fig. 9 Base wave at 25000 min^{-1}

Table 2 Compressor motor parameters

Motor Parameter	Value
Pole Pairs [-]	1
Phase Resistance [Ω]	0.205
Phase Inductance [mH]	0.300
Speed Constant [Vs/rad]	0.0013
Phase Voltage max. [V]	100
Phase Current max. [A]	17
Speed max. [min^{-1}]	150,000

parameters are crucial for the implementation of a motor control law.

The phase inductance showed a rotor angle dependability of 90°, which can be correlated to varying reluctance paths within the rotor assembly. An angle-dependent phase inductance due to reluctance variations is mainly known for Interior Permanent Magnet Synchronous Motors (IPMSM). This is the preferred PMSM type for high speed applications due to the resulting high centrifugal forces acting on the permanent magnets and because of the utilization of an additional reluctance torque due to rotor saliency [30, 31].

Figure 10 shows the so-called 'align and go' startup procedure originally used by the manufacturer with a rotor alignment phase, in which the rotor is brought into a known position. Thereafter, the accelerating torque can be applied. As a consequence, the base wave frequency gradually rises towards the desired rotational speed. This behavior can be observed in the figure, where a defined voltage vector is used initially to align the rotor, followed by an increase in frequency until the desired speed (25,000 min^{-1}) is reached. The procedure takes less than two seconds in total and shall likewise be implemented for the inverter.

The findings on the motor characteristics were fed into the development process in order to select an appropriate control scheme for the preliminary electronics design.

3.2 Control scheme

As stated in the motor characterization section, the compressor utilizes an IPMSM as its electrical drive. There are a set of different control strategies for PMSM [32–34]. One possibility is the Field Oriented Control (FOC) being widely used because of its efficiency, low torque ripple and superior dynamics [35]. Since the FOC relies on the transformation of values given in the stator reference frame into a rotor fixed coordinate system, the accurate rotor position has to be known. This position information can be measured using sensors on the rotor shaft or alternatively be determined by sensorless means.

Since the given compressor assembly does not allow an installation of a resolver, a sensorless rotor position estimation must be used. This is reasonable taking the possible loss moment of a resolver due to friction into account and

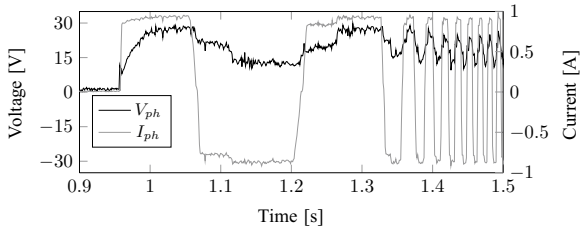

Fig. 10 Startup procedure

the challenge to use a resolver at the given rotational speed. Besides, system complexity is reduced and the stationary operating point at high speeds, which ensures a sufficient Back Electromotive Force (BEMF), is favorable for a sensorless control strategy.

Several methodologies for the sensorless rotor angle determination [32, 33] are practicable. Some methods rely on inductance variation effects resulting from a rotor-dependent magnetization variation, whereas others use the rotor-induced BEMF. Methods relying on the magnetization variations often use signal injection for the rotor position determination resulting in higher circuitry complexity [32]. A utilization of the BEMF only uses prevailing information such as phase voltage and current being already used within the FOC. Furthermore, this methodology is favorable because of the compressor-specific operating point at very high speeds.

One disadvantage of the BEMF methodology lies in the bad performance at low speeds and standstill, since no sufficient BEMF is generated within these points of operation. From standstill up to where a sufficient BEMF is induced, an open loop startup may be used. This can be implemented by setting the phase voltage depending on the mechanical frequency (u(f) characteristic). The initial rotor position, where the open loop acceleration will be started, can be implemented by the application of any but known voltage vector to the stator windings. The rotor is therefore aligned to a known position from which the base wave can be applied. Mode changes will be handled within a soft transition phase in accordance to the considerations made in Ref. [34].

Owing to the selected control scheme, being a sensorless FOC utilizing the generated BEMF, the phase current and voltages have to be measured. Those requirements were derived for the preliminary electronics design and will be discussed in the following section.

3.3 Design of preliminary electronics

Based on the preceding considerations, preliminary electronics were designed. This included the selection and analysis of suitable components and the composition of a system architecture. Main design drivers are the required switching frequencies, calculating execution time, the needed output power and the spatial restrictions together with the harsh environmental conditions. As stated in the stakeholder and overall requirements (Sect. 2.1), the electronics will utilize a 28 VDC supply for the low voltage components and 270 VDC for the power stage. The electronic components require a specific voltage levels, which will be converted from the low voltage supply using several buck regulators.

To properly modulate the base wave, a sufficiently high Pulse Width Modulation (PWM) switching frequency has to be chosen. It usually lies magnitudes over the base wave

frequency. The corresponding power electronics have to be able to drive the needed frequencies as well as to measure control relevant values, calculate the control loop and pass the desired pulse widths to the PWM modules. With higher electrical speeds, the requirements for calculation execution time and switching delay rise.

The motor to be controlled will run at a maximum speed of 150,000 min^{-1} as stated in Table 2. This corresponds to a base wave frequency for a motor with one pole pair of 2.5 kHz. A reasonable switching frequency of 100 kHz, which would result in 40 pulses per revolution, was chosen. Considering a desired regular sampling, meaning for every pulse a new desired value from the current control loop shall be available, the measurement circuitry and control loop calculation must run at the same frequency. A faster processing of the control loop is not reasonable since the controller can only influence the plant via the duty cycle of the PWM [32]. The developed preliminary electronics architecture is shown in Fig. 11.

A central component is the processor (TI C2000), which receives commands, such as the desired motor speed and sends out feedback data (e.g. phase currents and voltages) via a Controller Area Network (CAN) or Ethernet (ETH) interface. Based on the control law implemented on the processor, a PWM signal for each motor phase is generated, which is in turn amplified by the gate drivers (GD) to drive the semiconductors on the power stage (PS). Phase currents and voltages will be determined by sensors within the supply lines to the compressor motor. The electronics are supplied by 270 VDC (V_{DC}) and 28 VDC (V_{LV}), where buck converters (Buck) control the voltages down to the levels required for the components. Programming of the processor is achieved by an RS232 interface (RS).

To meet the requirements concerning the control loop timing, switching signal generation and realization of the

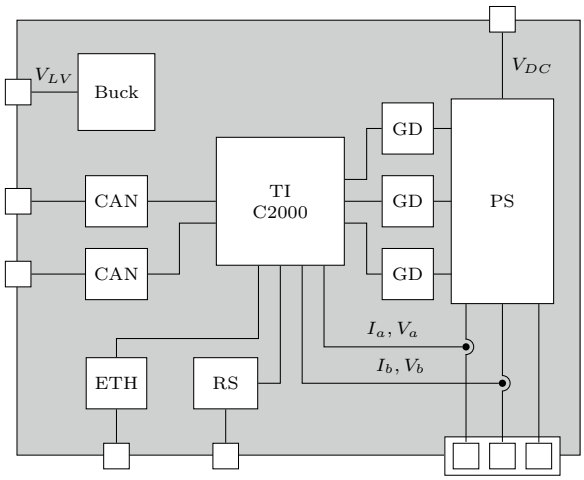

Fig. 11 Preliminary electronics architecture

required connectivity, a Digital Signal Processor (DSP) of the C2000 family was considered suitable for this application. A dual-core architecture enables a partitioned processing of less time-critical peripheral connectivity tasks and time-critical control loop algorithms. To fulfill the requirements of the regular sampling, a calculation time of < 5 µs for the control loop is needed. Implementations with the DMC library of Texas Instruments demonstrated a fast current control loop calculation time of < 1 µs [36]. Furthermore, the DSP enables a model-based software development approach using MATLAB Simulink and the corresponding support packages.

As far as the power stage is concerned, different approaches for the implementation were evaluated. This includes the composition from discrete semiconductors, integrated half bridges and integrated power modules. Due to the spatial restrictions together with a sophisticated thermal design of the integrated power modules, the latter was considered to be the best solution for this particular case. The CoolSiC™ technology, especially the power module FS45MR12W1M1_B11 from Infineon with a nominal current of $I_{D,nom}$ = 25 A and a breakdown voltage of V_{DS} = 1200 V indicated in the data sheet, was chosen to be implemented. Due to the desired switching frequency range, the resulting propagation delay had to be evaluated. At 100 kHz switching frequency the signal period is 10,000 ns. The accumulated propagation delays of the power module consisting of turn-on delay, rise time, turn-off delay and fall time adding up to 70.2 ns, which make up 0.7 % of the signal period and can be neglected.

The delay times of the gate drive circuitry are at higher magnitudes compared to the semiconductor devices. Suitable gate drivers have propagation delays of 70-500 ns. This is still no point of concern since the total delay will still be in the low single-digit percentage area in relation to the signal period. The gate drivers are selected considering the minimization of propagation delay and spatial efficiency.

The control strategy selected in Sect. 3.2 requires a measurement of at least two phase currents. Because of the high inverter voltage operation, it was decided that the data acquisition is implemented as galvanically isolated inline measurement using a current transducer. The GO 30-SMSSP3 from LEM was considered adequate because of the galvanic isolated measurement with a small outline and high bandwidth of 300 kHz. For the phase and dc-link voltage measurement, differential isolated operational amplifiers with corresponding voltage dividers are included into the design.

3.4 Thermal considerations

Another aspect considered within the selection process of the power semiconductor module is the thermal dissipation of the power electronics. The FS45MR12W1M1_B11 data

sheet contains the values being crucial for an initial estimation. In general, the dissipated heat mainly results from the drain-source resistance ($R_{DS,\,on} = 59\,m\Omega$) of the semiconductors as well as energy losses due to the switching ($E_{on} = 0.37$ mJ and $E_{off} = 0.035$ mJ), which depend on the switching frequency f_{sw} (100 kHz). Considering the maximum phase current I_{ph} (17 A root mean square) as stated in Table 2 and a number of six semiconductors on the power module, the total power loss (P_l) is calculated as:

$$P_l = 2(\sqrt{2} \cdot I_{ph})^2 \cdot R_{DS,on} + 3 \cdot f_{sw}(E_{on} + E_{off}) = 189.7\ \text{W} \tag{1}$$

Taking into account the maximum power consumption indicated in Table 2 (5100 W), this corresponds to an efficiency of 96 % and is in line with literature values [37, 38]. The dissipated heat shall be removed by convective means. Therefore, the integrated power stage will be mounted to a plate incorporating cooling fins, which is located on the front surface of the inverter looking to the airstream (minimum airspeed ≈10 m/s) of the compressor inlet to promote cooling efficiency. It can be assumed that the sucked in air will be near the ambient temperature. For HLFC design purposes, a maximum temperature of −30 °C is specified for the operation in cruise. On the other hand, the power module can withstand temperatures up to 150 °C. A de-rating of 20 % is applied in the preliminary design, so that 120 °C shall not be exceeded on continuous operation.

However, due to thermal resistances between the semiconductor junction and heat sink, the cooling plate will have a lower temperature than the power module. The temperature difference (ΔT_{JH}) in steady-state can be estimated as proposed in Ref. [39] using the thermal impedance between junction and heat sink ($Z_{th,JH} = 1.54$ K/W) and assuming an equal distribution of the power loss among the semiconductors

$$\Delta T_{JH} = \frac{P_l}{6} \cdot Z_{th,JH} \approx 49\ \text{K} \tag{2}$$

Hence, the cooling plate temperature shall not exceed 71 °C to ensure that the power module will operate within its temperature limit. The convection to dissipate the power loss via the cooling area A can then generally be described by:

$$P_l = h_c \cdot A \cdot \Delta T = h_c \cdot A \cdot (71\,^\circ\text{C} - (-30\,^\circ\text{C})) \tag{3}$$

The convective heat transfer is represented by h_c and strongly depends on the flow conditions around the cooling surface. In this case, the airflow from the compressor generates a forced convection enabling an increase in h_c. For simplification, the cooling area is regarded as a flat plate. Moreover, laminar flow is assumed as the calculated Reynolds number ($Re = 1.88 \times 10^4$) is below the critical value of 5×10^5 for the cooling system design case at maximum temperature (−30 °C) in cruise conditions. Several empirical equations, most of them listed in [40], exist to determine h_c. However, the used one corresponds to an isothermal flat plat at laminar flow is

$$\frac{h_c \cdot L}{k} = 0.664 \cdot Re^{0.5} \cdot Pr^{1/3} \tag{4}$$

where L represents the characteristic length, k the thermal conductivity and Pr the flow-related Prandtl number. Taking into account of the boundary conditions at the inverter's front surface (100 × 250 mm) used for the cooling, a value of $h_c = 20\,\text{W/(m}^2\text{K)}$ was calculated. Due to the low air density in cruise conditions, this is considerably lower to what can be expected at ground level.

Hence, a required cooling area of 0.093 m^2 can be specified by inserting all information in Eq. (3). Heat dissipation is only possible by one cooling surface (max. 100 × 250 mm) connected to the power module as all other surfaces are covered by surrounding structures. Therefore, it is obvious that fins are indeed required. Estimating the distribution of fins having a width of 3 mm and the same amount of clearance in between, a total number of 16 fins (n_f) can be realized along the cooling surface (width W = 100 mm, length L = 250 mm). In this way, the equation to determine the cooling area A in dependence on the fin height H by simple geometric relations can be defined.

$$A = 0.093\ \text{m}^2 = W \cdot L + 2 \cdot n_f \cdot L \cdot H \tag{5}$$

Thus, the value for H can be calculated as 8.5 mm. Taking the allowable space allocation into account, this seems feasible on a preliminary basis, even when adding uncertainty margins.

To validate the considerations, a thermal model including the dissipated power loss as well as the thermal mass of the cooling plate and the heat dissipation by convection was developed. The input values were taken from the power module's datasheet, calculations given in this paper and initially estimating aluminum as a material for the cooling plate. The simulation result in Simscape™ is shown in Fig. 12.

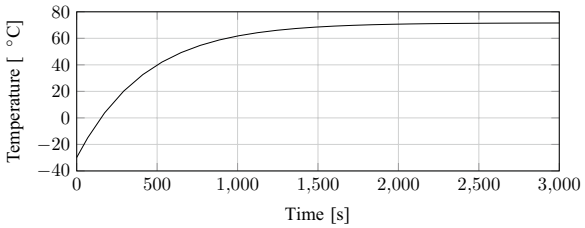

Fig. 12 Result of thermal simulation in Simscape™

Starting from the ambient temperature of −30 °C, the cooling plate reaches a temperature of 71 °C in steady-state. Therefore, the calculations made before comply with the simulation. Considering the estimated temperature difference between the cooling plate and semiconductor junction, the power module ought be operated within the designated limits. It has to be noted that this study has a preliminary character and is based on simplifications. A verification will be achieved in future by conducting tests in a climate chamber, which can also alter the ambient air pressure.

3.5 Experimental testbed

For feasibility testing an experimental testbench was constructed replicating the desired inverter configuration as stated in Sect. 3.3. The testbed includes an evaluation board of the desired integrated power stage with the corresponding drive and inline current measurement circuitry (CoolSiC™) (see schematic in Fig. 13).

3.6 Verification

A generic controller board is connected to the CoolSiC™ board, which comprises the embedded processor TMS320F28379D from the C2000 family of Texas Instruments (MC) providing the needed processing power, measurement circuitry as well as the desired connectivity functions. A dSpace system is used and acts together with the Host PC as a human-machine interface to communicate and command the embedded system via a CAN interface. The system also allows data acquisition for post-testing analysis. Moreover, the PC is used for programming the embedded electronics via RS232 or JTAG (Joint Test Action Group). The power stage is supplied by a 10 kW 270 VDC power supply, whereas a low voltage 28 VDC supply provides power to the MC.

Verification activities have been conducted to demonstrate proper function of the power electronics and corresponding measurement circuitry, which form the basis for further implementation and testing of the desired control algorithms. The tests were conducted with load resistors connected to the power outputs. This also allowed the determination of the propagation delay between the PWM signal of the DSP and the actual switching characteristics of the gate driver circuitry and semiconductor devices. The determined propagation delay was about 160 ns, which is reasonable regarding to the previous considerations. The testbed was operated up to maximum current and correct operation was demonstrated throughout the operational range.

Starting from the successful operation of the experimental testbed, the next steps within the development will be the implementation and verification of the control algorithms together with the development of a miniaturization of the testbed's electronics fulfilling the spatial requirements. The miniaturized prototype will then be verified against the demanded requirements as stated.

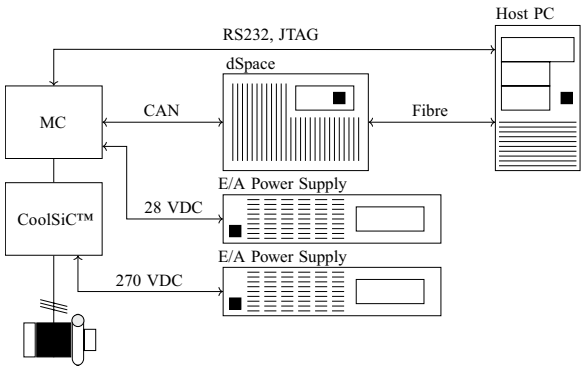

Fig. 13 Experimental testbed block diagram

4 Conclusion and outlook

Implementing HLFC on an aircraft comprises several challenging aspects. Essential key components are the compressor and the corresponding inverter, which are both on the edge of technical feasibility. Moreover, the operation in an aviation environment requires certain procedures to be followed in the development. An MBSE approach was applied in Cameo Systems Modeler to prepare the inverter design. Initially, basic requirements and relevant guidelines were identified. Thereafter, system functions were elaborated and linked to a logical architecture, leading to a first solution architecture. This in turn could be used to conduct the crucial safety assessments, as laid down in the ARP4754A, in order to include safety requirements. In the end, the list of requirements was validated for completeness and correctness, so that an adequate physical architecture could be defined.

Subsequently, the component development phase could be initiated. As the motor characteristics of the compressor were unknown, measurements have been conducted for elaborating a control concept and preliminary electronics design. Due to the challenges arising from the high rotational speed, it was aimed to assure that the inverter is able to drive the compressor in a first step. For this reason, a testbed was built up and used for verification neglecting requirements such as the integration of an AFDX interface. First tests are promising and assumptions made before, such as the delay times, comply with the measurements made.

Future work will comprise the miniaturization of the demonstrated electronics and initial tests in a climate chamber. After that, all features will gradually be implemented

and verified against the defined requirements. Because of the use of an MBSE model, the verification process can easily be carried out and adapted to the current project status.

Acknowledgements This project has received funding from the Clean Sky 2 Joint Undertaking (JU) under grant agreement CS2-LPA-GAM-2020-2023-01. The JU receives support from the European Union's Horizon 2020 research and innovation programme and the Clean Sky 2 JU members other than the Union.

Disclaimer The results, opinions, conclusions, etc. presented in this work are those of the author(s) only and do not necessarily represent the position of the JU; the JU is not responsible for any use made of the information contained herein.

Funding Open Access funding enabled and organized by Projekt DEAL. Open Access funding enabled and organized by Projekt DEAL.

Availability of data and materials Not applicable.

Code availability Not applicable.

Declarations

Conflict of interests The authors have no competing interests to declare that are relevant to the content of this article.

References

1. ACARE: Time for change: The need to rethink Europe's Flight-Path 2050 (2020)
2. Kilian, T., Horn, M.: Verification of a chamberless HLFC design with an outer skin of variable porosity. CEAS Aeron. J. **12**(4), 835–845 (2021). https://doi.org/10.1007/s13272-021-00528-4
3. Henke, R.: The Airbus A320 HLF Fin programme. Nouv. Rev. Aeronaut. Astronaut. **209**(2), 53–55 (1998)
4. Schrauf, G., von Geyr, H.: Hybrid laminar flow control on A320 fin: Retrofit design and sample results. J. Aircr. **58**(6), 1272–1280 (2021). https://doi.org/10.2514/1.c036179
5. Mosca, V., Karpuk, S., Sudhi, A., Badrya, C., Elham, A.: Multidisciplinary design optimisation of a fully electric regional aircraft wing with active flow control technology. Aeron. J. **126**(1298), 730–754 (2021). https://doi.org/10.1017/aer.2021.101
6. Beck, N., Landa, T., Seitz, A., Boermans, L., Liu, Y., Radespiel, R.: Drag reduction by laminar flow control. Energies **11**(1), 252 (2018). https://doi.org/10.3390/en11010252
7. Sudhi, A., Elham, A., Badrya, C.: Coupled boundary-layer suction and airfoil optimization for hybrid laminar flow control. AIAA J. **59**(12), 5158–5173 (2021). https://doi.org/10.2514/1.j060480
8. Barklage, A., Römer, U., Bekemeyer, P., Bertram, A., Himisch, J., Radespiel, R., Badrya, C.: Analysis and uncertainty quantification of a hybrid laminar flow control system. In: AIAA SCITECH 2022 Forum, San Diego, CA, USA and virtual (2022). https://doi.org/10.2514/6.2022-2452
9. Pohya, A.A., Wicke, K., Kilian, T.: Introducing variance-based global sensitivity analysis for uncertainty enabled operational and economic aircraft technology assessment. Aerosp. Sci. Technol. **122**, 107441 (2022). https://doi.org/10.1016/j.ast.2022.107441
10. Krishnan, K.S.G., Bertram, O.: Preliminary design and system considerations for an active hybrid laminar flow control system. Aerospace **6**(10), 109 (2019). https://doi.org/10.3390/aerospace6100109
11. HLFC-Win project website. www.hlfc-win.eu/. Accessed 22 Jun 2021
12. Fröhlich, P.: Development of an oil free turbo compressor for mobile fuel cell applications –challenges and results. In: Fuel cell conference FC^3, Chemnitz, Germany (2019)
13. Langmaack, N., Lippold, F., Hu, D., Mallwitz, R.: Analysing efficiency and reliability of high speed drive inverters using wide band gap power devices. Machine **9**(12), 350 (2021). https://doi.org/10.3390/machines9120350
14. Fleming, C.H., Leveson, N.: Improving hazard analysis and certification of integrated modular avionics. J. Aerosp. Inf. Syst. **11**(6), 397–411 (2014). https://doi.org/10.2514/1.i010164
15. SAE International. ARP4754A: Guidelines for development of civil aircraft and systems. SAE Int. (2010). https://doi.org/10.4271/arp4754a
16. Krupa, G.P.: Application of agile model-based systems engineering in aircraft conceptual design. Aeron. J. **123**(1268), 1561–1601 (2019). https://doi.org/10.1017/aer.2019.53
17. Mathew, P.G., Liscouet-Hanke, S., Masson, Y.L.: Model-based systems engineering methodology for implementing networked aircraft control system on integrated modular avionics – environmental control system case study. In: sae aerospace systems and technology conference, London, United Kingdom (2018). https://doi.org/10.4271/2018-01-1943
18. Andersson, H.: Aircraft systems modeling: Model based systems engineering in avionics design and aircraft simulation. Linköping University Electronic Press, Linköping (2009)
19. Walden, D., Roedler, G., Forsberg, K., Hamelin, R., Shortell, T. (eds.): INCOSE systems engineering handbook. Wiley, Hoboken (2015)
20. EASA: Certification specifications and acceptable means of compliance for large aeroplanes CS-25. Amendment 26 (2020)
21. SAE International. ARP4761: Guidelines and methods for conducting the safety assessment process on civil airborne systems and equipment. SAE Int. (1996). https://doi.org/10.4271/arp4761
22. RTCA: DO-160G-Environmental conditions and test procedures for airborne equipment (2010)
23. RTCA: DO-178C-Software considerations in airborne systems and equipment certification (2012)
24. RTCA: DO-254-Design assurance guidance for airborne electronic hardware (2000)
25. Horn, M., Seitz, A., Schneider, M.: Novel tailored skin single duct concept for HLFC Fin application. In: Proceedings of the 7th European Conference for Aeronautics and Space Sciences, Milano, Italy (2017)
26. Quanterion solutions incorporated: Non-Electronic Parts Reliability Data 2016, NPRD (2016)
27. Leveson, N., Wilkinson, C., Fleming, C., Thomas, J., Tracy, I.: A Comparison of STPA and the ARP 4761 safety assessment

process. MIT Technical Report, Massachusetts institute of technology (2014)
28. Thomas, J., Sgueglia, J., Suo, D., Leveson, N., Vernacchia, M., Sundaram, P.: An integrated approach to requirements development and hazard analysis. In: SAE 2015 World Congress & Exhibition, Detroit, MI, USA (2015). https://doi.org/10.4271/2015-01-0274
29. OMG ®: Risk Analysis and Assessment Modeling Language (RAAML). Version 1.0 Beta (2020)
30. Murakami, H., Honda, Y., Kiriyama, H., Morimoto, S., Takeda, Y.: The performance comparison of SPMSM, IPMSM and SynRM in use as air-conditioning compressor. In: Conference record of the 1999 IEEE industry applications conference. Thirty-forth IAS annual meeting (Cat. No.99CH36370), Phoenix, AZ, USA (1999). https://doi.org/10.1109/ias.1999.801607
31. Jahns, T.M., Kliman, G.B., Neumann, T.W.: Interior permanent-magnet synchronous motors for adjustable-speed drives. IEEE Trans. Ind. Appl. **IA–22**(4), 738–747 (1986). https://doi.org/10.1109/tia.1986.4504786
32. Schröder, D.: Elektrische Antriebe - Regelung Von Antriebssystemen. Springer, Berlin/Heidelberg (2015)
33. Kunzler, R.: Rotorlagegeberlose Verfahren zum Betrieb einer permanenterregten Synchronmaschine im elektrifizierten Antriebsstrang. PhD thesis, Otto-von-Guericke-Universität Magdeburg (2018)
34. Kiel, J.: Regelung permanenterregter Synchronmaschinen ohne mechanischen Geber für den industriellen Einsatz. PhD thesis, Universität Paderborn (2005)
35. Casadei, D., Filippetti, F., Rossi, C., Stefani, A.: Magnets faults characterization for permanent magnet synchronous motors. In: IEEE International symposium on diagnostics for electric machines, power electronics and drives. , Cargese, France (2009). https://doi.org/10.1109/demped.2009.5292770
36. Ramamoorthy, R.T.: Quick response control of PMSM using fast current loop. Technical report SPARCL1B, Texas Instruments (2019)
37. Muller, J.-K., Mertens, A.: Power electronics design for a direct-driven turbo compressor used as advanced high-lift system in future aircraft. In: IECON 2017 - 43rd Annual Conference of the IEEE Industrial Electronics Society, Beijing, China (2017). https://doi.org/10.1109/iecon.2017.8216756
38. Antivachis, M., Dietz, F., Zwyssig, C., Bortis, D., Kolar, J.W.: Novel high-speed turbo compressor with integrated inverter for fuel cell air supply. Front. Mech. Eng. (2021). https://doi.org/10.3389/fmech.2020.612301
39. Infineon technologies: Dynamic thermal behavior of MOSFETs: simulation and calculation of high power pulses. Application note AN_201712_PL11_001 (2017)
40. Sartori, E.: Convection coefficient equations for forced air flow over flat surfaces. Sol. Energy **80**(9), 1063–1071 (2006). https://doi.org/10.1016/j.solener.2005.11.001